ACS Catalysis

Research Article

pubs.acs.org/acscatalysis

Kinetic and Mechanistic Study of Glucose Isomerization Using Homogeneous Organic Brønsted Base Catalysts in Water

Jack M. Carraher, Chelsea N. Fleitman, and Jean-Philippe Tessonnier*

Department of Chemical and Biological Engineering, Iowa State University, Ames, Iowa 50011, United States

NSF Engineering Research Center for Biorenewable Chemicals (CBiRC), Ames, Iowa 50011, United States

Supporting Information

ABSTRACT: The isomerization of glucose to fructose represents a key intermediate step in the conversion of cellulosic biomass to fuels and renewable platform chemicals, namely, 5-hydroxymethyl furfural (HMF), 2,5-furandicarboxylic acid (FDCA), and levulinic acid (LA). Although both Lewis acids and Brønsted bases catalyze this reaction, the base-catalyzed pathway received significantly less attention due to its lower selectivity to fructose and the poor yields achieved (<10%). However, we recently demonstrated that homogeneous organic Brønsted bases present a similar performance (~31% yield) as Sn-containing beta zeolite, a reference catalyst for this reaction. Herein, we report on the first extensive kinetic and mechanistic study on the organic Brønsted base-catalyzed isomerization of glucose to fructose. Specifically, we combine kinetic experiments performed over a broad range of conditions (temperature: 80−120 °C; pH 9.5−11.5; reactant: glucose, fructose) with isotopic studies and in situ ^{1}H NMR spectroscopy. Pathways leading to isomerization and degradation of the monosaccharides have been identified through careful experimentation and comparison with previously published data. Kinetic isotope effect experiments were carried out with labeled glucose to validate the rate-limiting step. The ex situ characterization of the reaction products was confirmed using in situ ^{1}H NMR studies. It is shown that unimolecular (thermal) and bimolecular (alkaline) degradation of fructose can be minimized independently by carefully controlling the reaction conditions. Fructose was produced with 32% yield and 64% selectivity within 7 min.

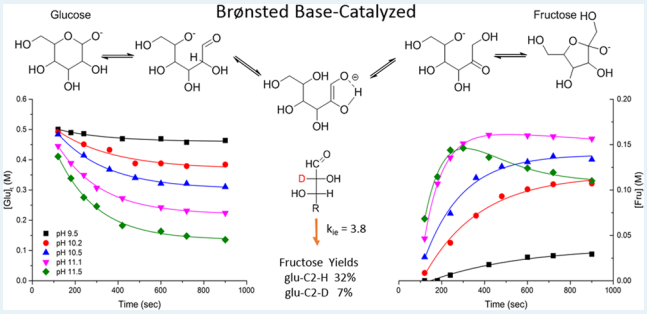

KEYWORDS: *glucose, fructose, base-catalyzed isomerization, Lobry de Bruyn−Alberda van Ekenstein, mechanism, kinetics, proton transfer*

INTRODUCTION

The isomerization of glucose to fructose represents an important industrial conversion for food applications (high fructose corn syrup) and is currently regarded as a key intermediate step in the production of platform chemicals from biorenewables, namely, 5-hydroxymethylfurfual (HMF), 2,5-furandicarboxylic acid (FDCA), and levulinic acid (LA).[1−3] These biobased building blocks are notably central to the production of plastics, green solvents, lubricants, and valeric biofuels.[1−3] The industrial state-of-the-art for the large-scale production of high fructose corn syrup currently utilizes immobilized enzymes (D-xylose isomerase) as a biocatalyst.[4−6] Fructose yields of 42% are obtained by this method,[6] which operates near thermodynamic equilibrium.[7] However, the enzymatic system suffers from a relatively short half-life[6] and requires the careful control of pH, temperature, feedstock purity, and flow rate to prevent any irreversible catalyst deactivation through microbial growth and/or thermal degradation.[4−6] There is, therefore, an ongoing search for robust high performance chemical catalysts that could replace costly enzymes. To be considered for both food applications and the production of renewable chemicals, these new catalysts should meet the following criteria: (i) guarantee a maximum level of isomerization with a minimum of reaction byproducts, (ii) be environmentally safe and nontoxic, (iii) be synthesized at a large scale and low cost, (iv) be easily separated from the product stream, and (v) be reusable without significant loss in performance.[8]

Zhao et al. reviewed a broad range of homogeneous and heterogeneous chemical catalysts active for the isomerization of glucose to fructose, including aqueous inorganic hydroxides, organic bases, alkali cation-exchanged zeolites, hydrotalcites, anion exchange resins, lanthanide salts, tin-containing beta-zeolite (Sn-β), and others.[9] Many catalysts offer a high selectivity to fructose but often at the expense of low glucose conversion. Additionally, leaching of caustic species, difficult and/or expensive catalyst syntheses and/or regeneration, as well as costly separation from product streams and waste disposal are frequently a concern.[9] Lewis acids, and in particular Sn-β, emerged as promising carbohydrate isomerization

Received: February 13, 2015
Revised: April 14, 2015

DOI: 10.1021/acscatal.5b00316
ACS Catal. 2015, 5, 3162−3173

Scheme 1. Glucose to Fructose Isomerization Pathways Proposed for Sn-β: Intramolecular Hydride Shift at Framework Sn (Right) or by Deprotonation at α-C and Proton Transfer through an Enediol Intermediate at Extra-Framework SnO_2 in Hydrophobic Pores (Left)[a]

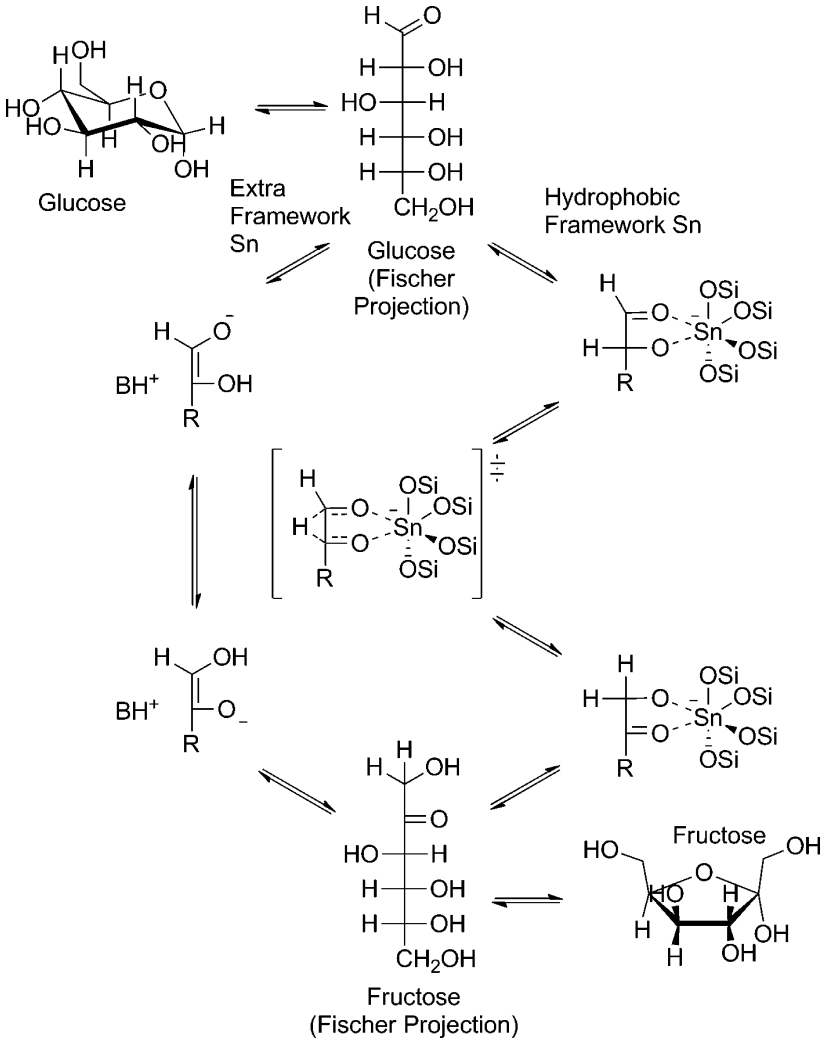

[a]Adapted from ref 18.

catalysts.[2,10−17] Sn-β isomerizes glucose to fructose with high selectivity (51%) and yields of up to 31%.[10] The reacted solution typically contains ∼84% of carbohydrates (glucose, fructose, mannose) and ∼16% of carboxylic acids and other byproducts formed through retro-aldol reactions of sugars.[11,13] Several studies aimed at elucidating the mechanisms involved in the Sn-catalyzed isomerization reaction have been carried out.[11−13,18,19] Framework tetrahedral Sn and extraframework octahedral Sn species (SnO_2) were both shown to catalyze the isomerization of glucose to fructose.[12] However, NMR investigations using isotope labeled glucose (gluc-C2-D) demonstrated that while framework Sn catalyzes the intramolecular hydride shift from the C-2 to C-1 position, extraframework SnO_2 located within the hydrophobic pores of the zeolite promotes the isomerization through base-catalyzed proton transfer (Scheme 1).[12]

Brønsted bases represent another important class of catalysts for the isomerization of glucose to fructose.[9,20−32] Isomerization under strongly alkaline conditions, though, resulted in very poor selectivity to fructose. Fructose yields below 10%[9,10,18,20,21,26,30,33−38] were reported and were likely due to the degradation of monosaccharides under alkaline conditions, which is known to produce over 50 different byproducts (mostly sugar derived acids).[25,38,39] However, we recently achieved high fructose yield (32%) from glucose using organic amine catalysts.[27] To the best of our knowledge, only one other group has reported high yields of fructose using an organic basic catalyst in an aqueous environment.[40] We proposed that isomerization likely occurs via the Lobry de Bruyn−Alberda van Ekenstein (LdB−AvE) mechanism, first reported in 1895.[30,31,41] In this mechanism, the C-2 proton on the acyclic form of glucose is abstracted by a Brønsted base, resulting in the formation of an enediol intermediate, and followed by hydrogen transfer from O-2 to O-1 and protonation of C-1 (Scheme 2).

Many mechanistic studies have been undertaken to investigate one or multiple elementary steps involved in the base-catalyzed isomerization. These studies have focused on every aspect from ring opening[20,22,42−46] to overall saccharide degradation[33,38,47−53] to the nature of intermediates involved in both isomerization and degradation. However, many results were found to be inconsistent, and the elementary steps

DOI: 10.1021/acscatal.5b00316
ACS Catal. 2015, 5, 3162−3173

Scheme 2. Lobry de Bruyn–Alberda van Ekenstein (LdB–AvE) Mechanism for the Base-Catalyzed Isomerization of Glucose to Fructose

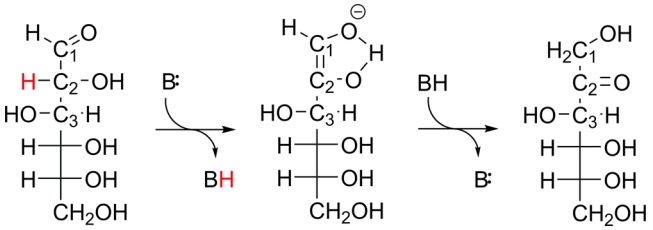

involved in the reaction have been a source of debate for over a century. The nature of the intermediate, for instance, has been called into question several times due to discrepancies between results obtained by different groups when using isotopically labeled sugars and/or solvents.[20,31,32,54,55] Although many of these investigations provide important clues about the mechanism of action, the overwhelming majority of these studies were performed under conditions that favor the formation of various byproducts, which probably explains the observed discrepancies.[30,31] The nature of the intermediate(s), the effect of pH and temperature on their formation, and the mechanisms involved in the degradation of the sugars are yet to be identified. Actually, true equilibrium concentrations of glucose and fructose have never been achieved with Lewis acid and Brønsted base catalysts due to the onset of degradation reactions.[10] Understanding the chemistry of carbohydrates as a function of temperature and pH is critical to identify the constraints that need to be considered for future catalyst design.

We report here on the first kinetic and mechanistic study for selective organic Brønsted base-catalyzed glucose–fructose isomerization. We recently demonstrated that organic Brønsted bases, specifically tertiary amines, catalyze the isomerization of glucose to fructose with high selectivity (63%) and yield (32%), a performance similar to the state-of-the-art Sn-β catalyst (51% selectivity, 31% yield).[27] We identified triethylamine (TEA) as an excellent candidate for further study based on its performance and lack of contribution to Maillard browning. The present work aims to develop an understanding of glucose isomerization and glucose/fructose degradation based on kinetics, kinetic isotope effect experiments, analysis of product distributions, and in situ ^{1}H NMR studies. The broad range of reaction conditions studied (temperature, number of active sites, glucose concentration, pH, ionic strength) allows us to propose for the first time a model that captures most of the key parameters: the kinetics of both glucose and fructose conversion, the degradation of fructose through unimolecular and bimolecular pathways, the effect of temperature and pH on the degradation pathways, the buffering effects of both sugars, and the effect of atmospheric CO_2. Reaction kinetics and kinetic isotope effect experiments point to the rate-limiting step. The calculated rate constants and thermodynamic parameters provide key information on conditions required to achieve high fructose yields.

MATERIALS AND METHODS

In a typical experiment, a 50.0 mL mother solution containing 0.56 ± 0.02 M (10 wt %) D-glucose (≥99.5%, Sigma-Aldrich) or D-fructose (≥99%, Sigma-Aldrich) was prepared with Ar-purged DI water (Barnstead Nanopure Infinity Pyrogen Free UF Laboratory Water System Model D8981) in a 100 mL round-bottom flask with olive shape stir bar. The mother solution was purged with Ar for an additional 20 min once dissolution of the sugar was complete. The pH was then measured (Mettler Toledo SevenMulti, InLab Routine Pro electrode) and adjusted to the desired initial pH by titration with triethylamine (≥99%, Sigma-Aldrich) using a syringe. The flask and the pH electrode were fitted with rubber septa to minimize introduction of atmospheric CO_2 which could cause deviations in pH due to formation of carbonic acid during the measurement. Eight 5.0 mL aliquots of the mother solution were then transferred via syringe to Ar-filled 5 mL thick-walled glass reactors (Chemglass Life Sciences) containing a V-shaped stir bar. The reactor vessels were then placed in the preheated 1 L oil bath (digital stirring hot plate IKA RCT equipped with PT1000 thermocouple in the oil bath). No more than eight vials were placed in the oil bath simultaneously to minimize the drop in temperature (~5 °C). Preliminary tests performed with an oil bath at 100 °C showed that the reaction mixture reaches the target temperature within ~120 s. The reactors were removed at set time intervals, and the reaction was quenched using an ice bath. All the reactors were later stored in a freezer until analysis. Analogous experiments were carried out with NaOH (99.8%, Fisher), piperidine (≥99%, Sigma-Aldrich), and pyrrolidine (≥99.5%, Sigma-Aldrich) for comparison. Deuterated glucose (C2-D) was purchased from Cambridge Isotope Laboratories, Inc. and used without any further treatment for the isotope exchange and kinetic isotope effect experiments. D_2O was supplied by Sigma.

For analysis, the frozen samples were brought to room temperature, diluted using appropriate amounts of 50:50 acetonitrile/water (HPLC grade, Fisher) containing 0.2 vol % TEA, and analyzed with a Waters Acquity H-Class ultra-performance liquid chromatograph (UPLC) equipped with photodiode array (PDA) and evaporative light scattering (ELS) detectors by methods analogous to those described previously (Supporting Information).[27] The instrument was calibrated before analyzing each set of samples (typically each day).

Kinetic traces were constructed and analyzed with Origin Pro 9.1 software (OriginLabs).

Yields are reported after 15 min (ca. 6.5 apparent half-lives at 100 °C relative glucose consumption) or after three apparent half-lives when studying temperature effects. Standard initial reaction conditions were 0.52 M glucose or fructose, pH_o 11 (12 ± 1 mol % TEA), and 100 °C. The effect of varying $[sugar]_o$, pH_o (mol % TEA), or temperature was determined while holding the other two variables constant at the above-described conditions. Byproduct yields are defined as the difference between the initial sugar concentration and the total sugar (glucose, fructose, and mannose) after 15 min (or three apparent half-lives when temperature was varied).

^{1}H NMR spectra were collected with a Bruker 600 MHz NMR (AVIII600). In order to study the rate of glucose conversion, a time-arrayed data set was acquired in which a single scan 1D proton spectrum was obtained at an interval of 5 s over the course of 1500 s. The temperature was regulated to 353.4 K during the acquisition.

RESULTS

We previously demonstrated that primary, secondary, and tertiary amines catalyze the isomerization of glucose to fructose with high yields, ranging between 15 and 32% depending on the chemical structure and pK_a of the base.[27] Primary and secondary amines were the least selective due to the formation

DOI: 10.1021/acscatal.5b00316
ACS Catal. 2015, 5, 3162–3173

of colored byproducts through the Maillard reaction, a nonenzymatic browning reaction well-known in food sciences.[56,57] UV−vis and ^{1}H NMR spectra confirmed that tertiary amines do not react and are not consumed by the Maillard reaction, in good agreement with the mechanism for this reaction.[58] Triethylamine was found to be the most promising homogeneous catalyst based on its high performance, availability, low toxicity, and low cost.[27,59,60] In addition, various triethylamine derivatives are commercially available, which offers many possibilities for the synthesis of the corresponding heterogeneous catalysts.

The experimental setup was further improved since our preliminary experiments. Various protocols were tested in order to increase the heating rate, lower the impact of atmospheric CO_2, and other possible artifacts. Aluminum heating blocks, which are commonly used for reactions with 5−10 mL reactors, were found to have a good heat conductivity but a relatively low heat capacity. Temperature dropped by approximately 10 °C when placing more than five vials at a time. Therefore, a conventional 1 L oil bath was preferred to perform kinetic studies as temperature dropped by only ∼5 °C and the reactors reached the target reaction temperature within ∼120 s. The conversion of glucose during heating is relatively negligible at pH_o 10.5 or below; however, at pH_o 11.5, nearly 17% conversion of glucose is observed by the first point of data collection (Figure 1). The experimental protocol was also improved in order to prevent any artifact due to atmospheric CO_2. Carbonic acid significantly impacts both selectivity and conversion (Supporting Information, Figure S1), and its effect varies depending on the base and pH of the reaction mixture. Therefore, all the reactions performed for the present work were carried out under Ar. Finally, small differences in glucose and fructose concentrations were measured when storing the reacted solutions in a fridge for more than 24 h, thus indicating that the reaction proceeds even at low temperature. However, the composition did not change when storing the reactors in a freezer, even for an extended period of time (1−2 weeks).

Isomerization from Glucose: Kinetics. The first few $[Glu]_t$ data points were used to construct linear $\ln([Glu]_t/[Glu]_o)$ versus t plots (eq 1) and observed first-order rate constants, k_{obs}, were obtained from the slope. The pH decreased during this time period but typically by less than 0.3 units. The observed first-order rate constant was found to be $9.3 \pm 0.9 \times 10^{-4}$ s^{-1} at pH_o 11.0 and showed no dependence on initial glucose concentration (Table 1), consistent with the kinetic traces previously reported under similar conditions.[40] The zero-order dependence of k_{obs} on [Glu] indicates that the process is unimolecular with respect to glucose, likely ring opening. k_{obs} showed an upward trend with pH_o (Figure 2). The apparent pH dependence on reaction kinetics suggests that ring opening most likely occurs from a deprotonated form of ring glucose.[20,24] As the reaction approached completion, the pH decreased dramatically (typically by 2−4 units). This likely results from the known degradation of sugars under alkaline conditions yielding acid products,[25,38,39] and as alluded to in our previous work,[27] is likely the leading factor in reversible catalyst poisoning. Finally, k_{obs} varied substantially with temperature (Table 2). The plot of $\ln(k_{obs}/T)$ versus $1/T$ shown in Figure 3 is linear and fits eq 2, where k_B is the Boltzmann constant, h is Planck's constant, R is the ideal gas law constant, and T is temperature in Kelvin. The slope and intercept provide activation parameters for glucose conversion $\Delta H^{‡}$ and $\Delta S^{‡}$ of 58 ± 8 kJ/mol and −144 ± 30 J/molK,

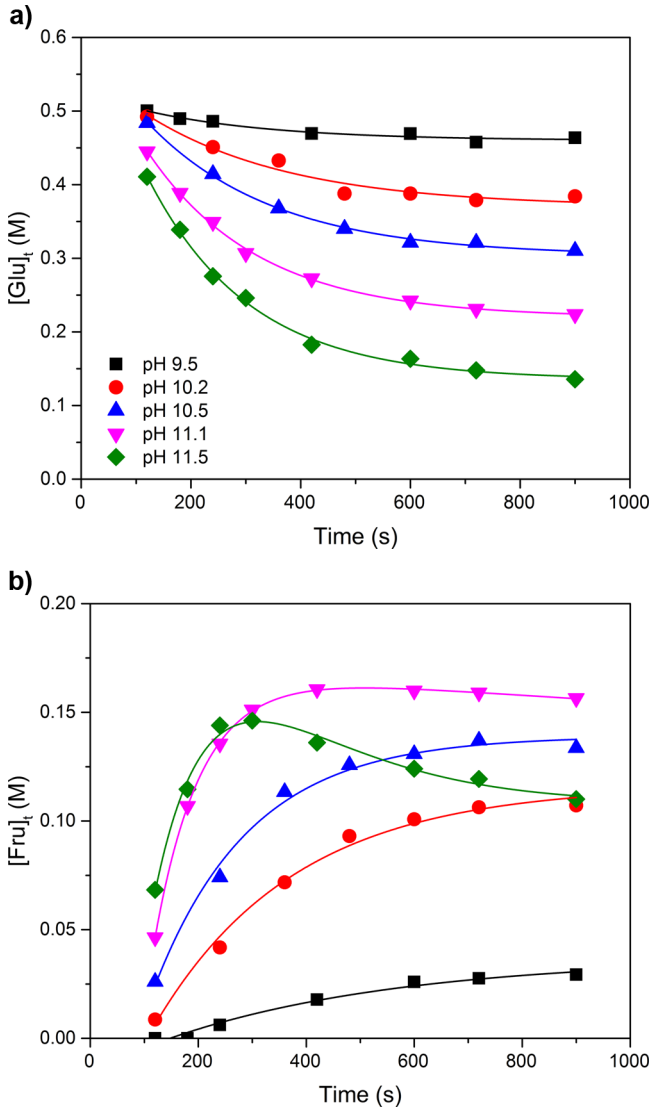

Figure 1. Plots of glucose (a) and fructose (b) concentrations as a function of time. Each data point corresponds to a single experiment. Reactions were carried out at 100 °C in degassed aqueous solutions of 0.52 M glucose with 0.03 ■, 1.29 red ●, 3.87 blue ▲, 12.24 pink ▼, and 108.68 green ◆ mol % TEA relative to glucose.

respectively (Table 3). Kinetic traces obtained from monitoring the formation of fructose were much more complicated, and they indicate fructose formation and decay on the same time scale (Figure 1). At the highest pH_o studied, fructose yields were observed to reach a maximum and then decay. The product distributions obtained from the above-described reactions are complicated by this degradation, and are discussed in detail in the next section, vide infra.

$$\ln\left(\frac{[Glu]_t}{[Glu]_o}\right) = -k_{obs} \times t \quad (1)$$

; where $[Glu]_t$ = glucose concentration at time t, $[Glu]_o$ = initial glucose concentration, k_{obs} = observed rate constant, and t = time in seconds.

$$\ln\left(\frac{k}{T}\right) = \ln\left(\frac{k_B}{h}\right) + \frac{\Delta S^{‡}}{R} - \frac{\Delta H^{‡}}{RT} \quad (2)$$

DOI: 10.1021/acscatal.5b00316
ACS Catal. 2015, 5, 3162−3173

Table 1. Effects of Glucose Concentration on Kinetics and Catalytic Performance[a]

entry	$[Glu]_o$ (M)	$10^4 \times k_{obs}$ (s^{-1})	pH_f	X_{Glu}[b]	Y_{Fru}[c]	Y_{Man}[d]	S_{Fru}[e]
1	0.288	8.4 ± 0.1	9.1	58	25	0	43
2	0.390	8.9 ± 0.1	9.9	56	26	5	46
3	0.521	10 ± 1	9.5	57	28	7	49
4	0.523[f]	14 ± 2	8.7	52	23[h]	4	44
5	0.523[g]	15 ± 1	9.3	49	24[h]	4	49
6	0.523[i]	10.9 ± 0.2	9.4	55	27	[j]	49
7	0.644	9.4 ± 0.2	9.9	56	27	6	47
8	0.746	8.6 ± 0.2	9.5	59	27	7	46
9	2.900	10.7 ± 0.2	9.9	64	21	6	33

[a]Standard reaction conditions: 100 °C, 0.52 M glucose, 12 ± 1 mol % TEA relative to glucose (pH_o 11.0), reactors quenched after 2, 3, 4, 5, 7, 10, 12, and 15 min. Conversion and yields reported to 1% error. Rate constants were determined by fitting eq 1 to the data. Conversion, yields, selectivity, and pH_f reported at 15 min reaction time. [b]Glucose conversion. [c]Fructose yield. [d]Mannose yield. [e]Fructose selectivity. [f]7.5 mol % piperidine (pH_o 11.0). [g]9.4 mol % pyrrolidine (pH_o 11.0). [h]Relatively low fructose yields and larger rate constants are likely due to participation of secondary amines in bimolecular Maillard browning (glu + R_2NH).[27] [i]12 mol % TEA with 0.1 M NaCl (ionic strength ca. 0.24 M). [j]Difficult to distinguish from baseline in UPLC.

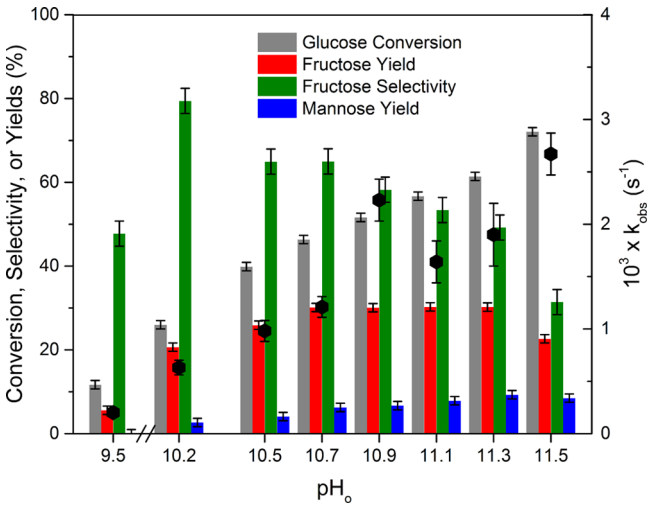

Figure 2. Conversion, selectivity, or yield (left axis) and k_{obs} (right axis) as a function of initial pH for glucose isomerization in the presence of TEA. Reactions were carried out at 100 °C in degassed aqueous solutions containing 0.52 M glucose and 0.03−108.68 mol % TEA relative to glucose.

Table 2. Effects of Temperature on Kinetics and Catalytic Performance[a]

temp (°C)	$10^4 \times k_{obs}$ (s^{-1})	X_{Glu}[b]	Y_{Fru}[c]	Y_{Man}[d]	S_{Fru}[e]
60	1.6 ± 0.2	26	14	2	52
80	5.6 ± 0.5	52	24	6	45
100	26 ± 1	51	28	6	56
120	39 ± 6	56	19	[f]	35

[a]Standard reaction conditions: 0.52 M glucose, 12 mol % TEA relative to glucose (pH_o 11.0). Rate constants were determined by fitting eq 1 to the data. Conversion and yields reported to 1% error. Conversion, yields, and selectivity are reported after three apparent half-lives. [b]Glucose conversion. [c]Fructose yield. [d]Mannose yield. [e]Fructose selectivity. [f]Difficult to distinguish due to noisy baseline in UPLC; however, earlier results suggest 7% mannose.[27]

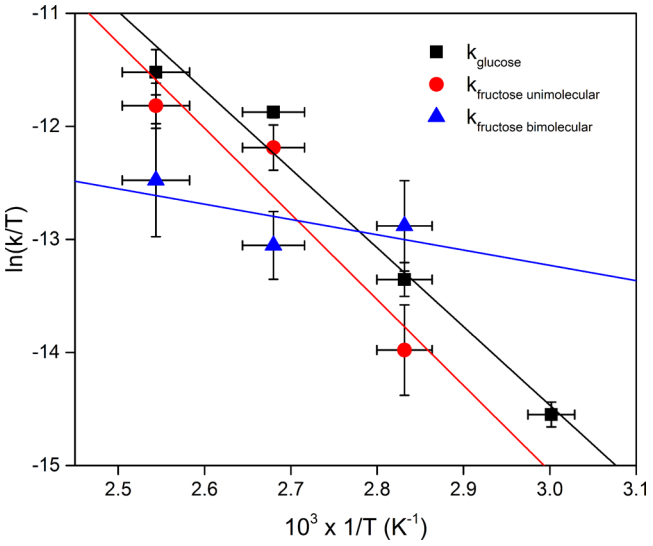

Figure 3. Effect of temperature on rate constants for glucose consumption, unimolecular fructose consumption, and bimolecular fructose consumption. $k_{fructose\ unimolecular}$ and $k_{fructose\ bimolecular}$ (for reactions 3 and 4) were determined from the *y*-intercept and slope, respectively, in the plot of k_{obs} vs $[Fru]_{ave}$ shown in Figure 5.

Table 3. Activation Parameters for Glucose Isomerization and Fructose Degradation[a]

reaction[a]	$\Delta H^{\ddagger}$ (kJ/mol)	$\Delta S^{\ddagger}$ (J/molK)	$E_{a100\ C}$ (kJ/mol)[e]
Glu_{unimol}[b]	58 ± 8	−144 ± 30	61
Fru_{unimol}[c]	63 ± 11	−134 ± 32	66
Fru_{bimol}[d]	11 ± 7	−274 ± 45	14

[a]Standard reaction conditions: 0.52 M glucose, 12 mol % TEA (pH_o 11.0). [b]Isomerization from glucose to fructose. k_{obs} obtained from eq 1 for glucose conversion. [c]Isomerization from fructose to glucose. k_{uni} obtained from *y*-intercept in Figure 5. [d]k_{bimol} obtained from the slope in Figure 5. [e]Activation energies were calculated from temperature and $\Delta H^{\ddagger} = E_a - RT$.

; where $k = k_{obs}$ obtained from eq 1, T = temperature in Kelvin, k_B = Boltzmann constant, h = Planck's constant, R = ideal gas constant, $\Delta S^{\ddagger}$ = entropy of activation, and $\Delta H^{\ddagger}$ = enthalpy of activation.

Isomerization from Glucose: Products. Variations in pH_o (9.5−11.5) when heating a 0.52 M glucose solution to 100 °C resulted in a linear increase in glucose consumption (Figure 2). Likewise, yields of mannose increased linearly with pH_o to a maximum of 9%. Fructose yields, however, showed a peculiar trend in that they rose steadily from 6% to 30% between pH 9.5 and 10.7, remained constant (30%) between pH 10.7 and 11.3, and then decreased to 23% at pH 11.5. The maximum yield of fructose obtained in this work was 32% (100 °C, pH_o 11.3, 7 min). Increasing the initial glucose concentration from 0.29 to 0.75 M had little to no effect on glucose conversion or fructose yield (Table 1). However, increasing glucose concentrations to 2.9 M (45 wt %) resulted in a decrease in fructose yield to only 21%. Factors like fructose degradation and buffering effects of the sugars must be considered when analyzing the product distribution of these very high [Glu] reactions. The multiple degradation pathways described below in conjunction with the long residence times (that is, the system being run in batch as opposed to flow reactors) likely work together to diminish yields at high [Glu].

DOI: 10.1021/acscatal.5b00316
ACS Catal. 2015, 5, 3162−3173

Isomerization from Fructose: Kinetics. Study of the reverse reaction (i.e., isomerization of fructose to glucose) resulted in similar trends (Figure 4). Like glucose, the first few

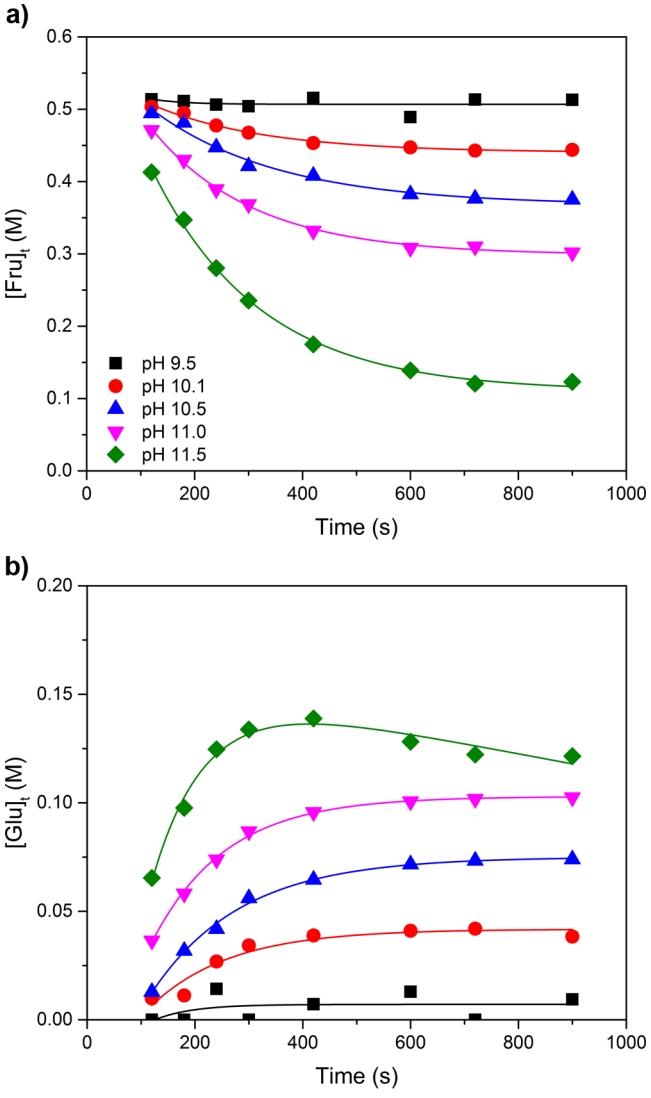

Figure 4. Plots of fructose (a) and glucose (b) concentrations as a function of time. Each data point corresponds to a single experiment. Reactions were carried out at 100 °C in degassed aqueous solutions of 0.52 M fructose with 0.03 ■, 1.14 red ●, 2.67 blue ▲, 9.67 pink ▼, and 67.98 green ◆ mol % TEA relative to fructose.

data points for fructose consumption fit eq 1, and k_{obs} increased with pH_o (Figure S2). However, k_{obs} for fructose consumption had a linear dependence on $[Fru]_{ave}$ (Figure 5). At the highest pH_o (11.5), kinetic traces monitoring formation of glucose reached a maximum and clearly decayed (Figure 4). Although similar to isomerization from glucose, this behavior was far less pronounced when fructose was the sugar initially present. The rate constants obtained from the reaction series in Figure 5 are shown in Table 4 and are indicative of unimolecular (*y*-intercept) and bimolecular (slope) reactions (eqs 3, 4). Rate constants obtained in the presence of NaOH in place of TEA were similar, therefore, reactant X in eq 4 is believed to be OH^-, vide infra. Additionally, under the conditions of these experiments, fructose is considered the excess reagent and OH^- the limiting reagent, as initially $[Fru]/[OH^-]$ = 520, and this

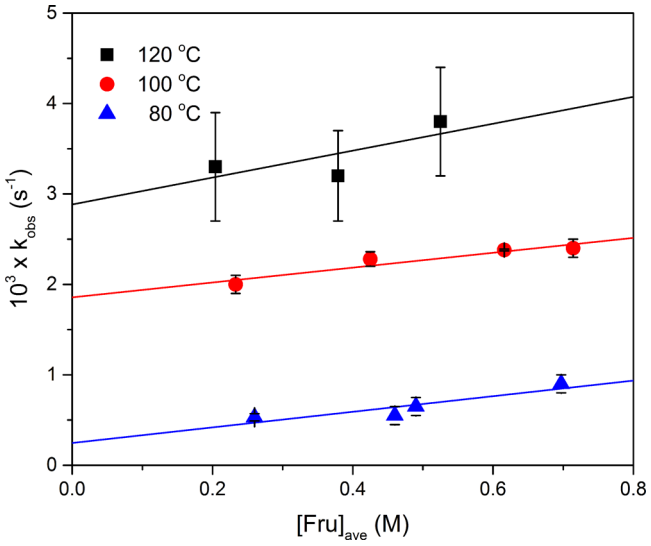

Figure 5. Plot of k_{obs} as a function of average fructose concentration: $[Fru]_{ave} = 1/2([Fru]_o + [Fru]_{240\,s})$. All reactions were carried out with an initial pH of 11.0 ± 0.1.

Table 4. Temperature Dependence of Rate Constants Obtained from Fructose Experiments

temp (°C)	$10^4 \times k_{unimol}$ (s^{-1})	$10^4 \times k_{bimol}$ (M^{-1} s^{-1})
80	3 ± 1	9 ± 3
100	19 ± 2	8 ± 2
120	29 ± 5	15 ± 10

ratio increases as OH^- is consumed. Therefore, the rate constant is expected to scale with [Fru]: $k_{obs} = k_{unimol} + k_{bimol} \times [Fru]_{ave}$. The activation parameters for these two reactions are shown in Table 3. Studies beginning with fructose were also attempted at 60 °C, but k_{obs} contained substantial error. Additionally, these reaction conditions were not studied in depth due to half-lives on the order of hours.

$$\text{Fructose}_{ring} \rightarrow \text{Products} \qquad k_{unimol} \qquad (3)$$

$$\text{Fructose}_{ring} + X \rightarrow \text{Products} \qquad k_{bimol} \qquad (4)$$

Isomerization from Fructose: Products. The product distributions obtained when beginning the isomerization from fructose (Figure S2) were more complicated likely due to the multiple reaction pathways observed kinetically (eqs 3, 4). Variations in temperature resulted in no discernible trend with regard to fructose conversion, Table 5 entries 3, 6, and 11 or entries 4, 8, and 12, but glucose yields clearly decrease with increasing temperature. The decrease in glucose yield at higher temperatures is most likely due to reactions other than isomerization of linear forms of the sugars, given the majority of k_{obs} is made up of the unimolecular process (Figure 5). In contrast, at 80 °C, where [Fru] has a significant effect on k_{obs}, the increase in glucose yields with [Fru] could suggest that at least some of the bimolecular pathway ultimately leads to glucose formation. The effect is also observed at 100 °C, albeit less pronounced, as k_{obs} at 0.5 M [Fru] is approximately 4:1 unimolecular/bimolecular.

Isomerization from Glucose: Kinetic Isotope Effects. Isomerization (pH_o 10.9, 100 °C) of glucose isotopically labeled at the C-2 position (glucose-C2-D) yielded $k_{obs} = 4.9 \pm 0.6 \times 10^{-4}$ s^{-1}. The corresponding kinetic isotope effect, k_{ie} =

DOI: 10.1021/acscatal.5b00316
ACS Catal. 2015, 5, 3162−3173

Table 5. Effects of Temperature and Concentration on Fructose Conversion at Three Apparent Half-Lives[a]

entry	$[Fru]_{ave}$[b] (M)	temp (°C)	$10^3 \times k_{obs}$ (s^{-1})	X_{Fru}[c]	Y_{Glu}[d]	Y_{Man}[e]	S_{Glu}[f]
1	0.260	80	0.53 ± 0.1	22	10	4	8
2	0.460	80	0.55 ± 0.1	46	24	7	52
3	0.490	80	0.65 ± 0.1	46	24	7	51
4	0.697	80	0.90 ± 0.1	50	28	3	56
5	0.233	100	2.0 ± 0.1	58	21	6	36
6	0.391[g]	100	2.0 ± 0.2	49	20	-[h]	41
7	0.425	100	2.3 ± 0.1	62	18	3	29
8	0.616	100	2.4 ± 0.1	47	24	9	51
9	0.714	100	2.4 ± 0.1	48	25	2	52
10	0.204	120	3.3 ± 0.6	52	18	5	34
11	0.379	120	3.2 ± 0.5	40	16	5	40
12	0.525	120	3.8 ± 0.6	45	17	5	38

[a]Standard reaction conditions: 12 ± 1 mol % TEA (pH_o 11.0), vary $[Fru]_o$ and temperature. Rate constants were determined by fitting eq 1 to the data. Product data reported after three apparent half-lives. [b]$[Fru]_{ave} = 1/2([Fru]_o + [Fru]_\infty)$. [c]Fructose conversion. [d]Glucose yield. [e]Mannose yield. [f]Glucose selectivity. [g]10 mol % NaOH (pH_o = 11.05). [h]Difficult to distinguish from baseline in UPLC.

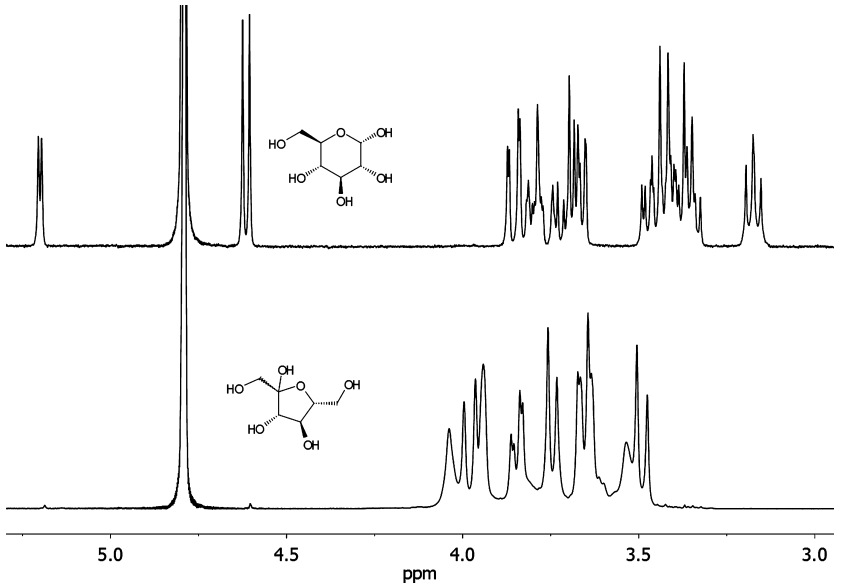

Figure 6. ^{1}H NMR spectra of glucose (*top*) and fructose (*bottom*) in the presence of TEA, 600 MHz, D_2O. TEA signals are omitted for clarity.

3.8, indicates that deprotonation of the C-2 position plays a substantial role in the in the conversion of the linear form of glucose. In addition, evidence for competitive reactions from linear glucose is easily seen when considering the product yields from glucose-C2-D relative to glucose−C2-H. Glucose conversion, fructose yields, and fructose selectivity (36%, 7%, and 20%, respectively) increased when replacing deuterated glucose-C2-D by glucose-C2-H (47%, 30%, and 64%, respectively). Mannose yields remained relatively unchanged at 5% (glu-D) and 6% (glu-H). Reactions with glu-H carried out in D_2O were identical in both kinetics and product distribution to those in H_2O, as indicated by the solvent kinetic isotope effect k_{ie} = 1. The solvent is therefore not expected to play a kinetically significant role as a proton donor (e.g., for the protonation of the saccharides) during isomerization.

Isomerization from Glucose: Products Formation and Kinetics by In Situ ^{1}H NMR. Glucose and fructose present several distinctive peaks in ^{1}H NMR spectra, which can be used to monitor changes in concentrations of both sugars during reaction (Figure 6). Reactions were carried out in J. Young tubes that were sealed under ambient temperature and pressure. The concentrations of the sugars were determined by integration of the following regions: fructose (2 H δ 4.25−4.35) and glucose (0.6 H δ 3.5−3.65) relative to TEA (9H δ 1.09) signals, used here as an internal standard. The time-resolved evolution of these signals and the in situ kinetic traces for the reaction of 0.5 M glucose and 12 mol % TEA (pD_o = 11.0) at 82 °C are shown in Figures 7 and 8. The shifts in peak positions observed during the first 66 s (Figure 7) are due to the increase in temperature from 22 to 82 °C. Interestingly, the onset of the fructose signal is slightly shifted compared to the glucose consumption (Figures 7 and 8). This shift could be due to integration errors arising from the signal/noise ratio of a broad fructose signal particularly obvious at low concentration.

^{1}H NMR spectra acquired at room temperature before and after reaction (Figure S3) only revealed peaks characteristic of the carbohydrates. Byproducts such as carboxylic acids were not observed directly, most probably because the concentration of each byproduct was below the detection limit of the technique. Room-temperature spectra acquired before and after reaction suggested a glucose conversion and fructose yield on the order of 23% and 17%, respectively. UPLC analysis of the same solution revealed 29% glucose conversion with 18% yield of fructose, thus confirming that NMR is a reliable technique to

DOI: 10.1021/acscatal.5b00316
ACS Catal. 2015, 5, 3162−3173

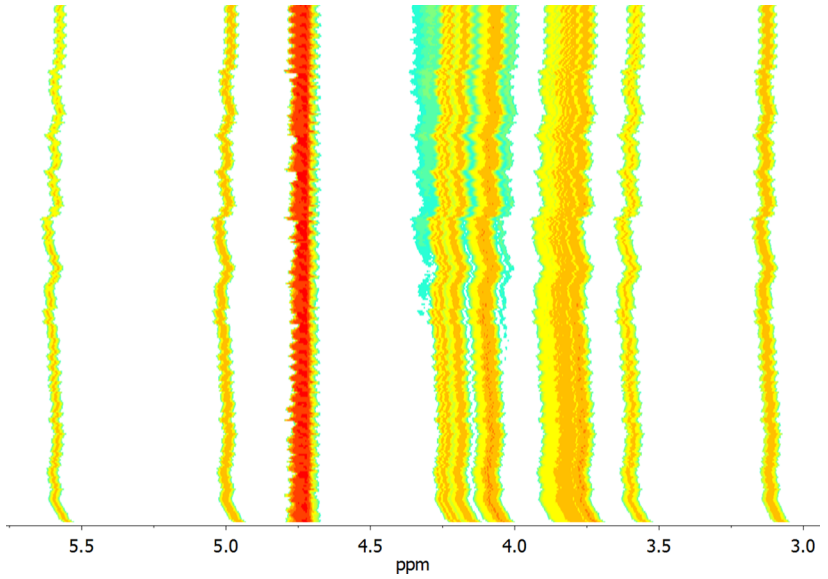

Figure 7. ^{1}H NMR in situ kinetics of 0.52 M glucose, 12 mol % TEA relative to glucose (pD_o = 11.0), 82 °C, 600 MHz, D_2O. Bitmap of ^{1}H NMR (horizontal) and time (vertical) from 0 (*bottom*) to 1500 s (~3 apparent half-lives, *top*). Blue signals at 4.00−4.05, 4.13−4.15, and 4.25−4.35 ppm correspond to fructose formation.

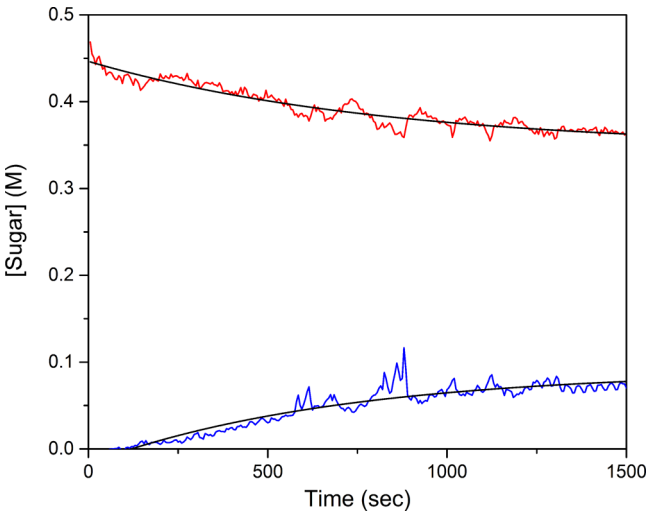

Figure 8. In situ ^{1}H NMR kinetic traces for 0.52 M glucose and 12 mol % TEA relative to glucose, 600 MHz, D_2O, 82 °C. Sugar concentrations (glucose: red —; fructose: blue —) were experimentally determined relative to TEA signals. The solid black lines are fits to equations for exponential decay.

quantify carbohydrates. However, these values are on the order expected for pD_o ~ 9.5−10.2. Analogous experiments carried out at pH 10.2 in 5 mL reaction vials and heated in the oil bath yielded a glucose conversion of 25% and fructose yield of 18% after 8 min at 100 °C. It appears that while ^{1}H NMR is a suitable method for determination of glucose conversion and fructose yield at room temperature, the use of TEA as the internal standard provides erroneous results due to its volatility at 82 °C and the significant difference in head space between 5 mL reaction vials (~0.5 mL head space) and a J. Young tube (2−3 mL head space). As a result [TEA] in solution is lower at elevated temperatures in a J. Young tube relative to the 5 mL reaction vials. This causes a decrease in pH and a false standard against which sugar signals are compared. For this reason and the necessity of remaining below the boiling point of D_2O, no further kinetic studies were done by NMR. Of interest, however, was (i) the validation that the same products are detected by NMR and UPLC and (ii) the possibility to use variations in chemical shifts of TEA signals as an in situ pH probe (Figure S4).

DISCUSSION

General Considerations. Due to limitations in experimental design and the complexity of the system, the observed rate constants obtained from kinetic traces monitoring the consumption of either glucose or fructose are at the very least composite rate constants for the reversible process (eq 5) and degradation reactions outlined in Scheme 4. Even at the lowest pH_o studied, ca. 7% of glucose was converted to products by the time the first data point was collect (120 s). By this time, both forward and reverse reactions were active and contributed to the observed rate constant. We were therefore unable to study the forward and reverse reactions independently. Additionally, considerations must be made for decomposition pathways and changes in pH under reaction conditions.

$$\text{Glucose} \underset{k_{\text{reverse}}}{\overset{k_{\text{forward}}}{\rightleftharpoons}} \text{Fructose} \qquad (5)$$

The thermodynamic maximum yield of fructose, based on glucose−fructose equilibrium, is 57.4% at 100 °C (does not take into account the formation of mannose).[7] However, both our previous[27] and current work indicate glucose conversions far beyond that (75%) and fructose yields well below 57% (32%). Clearly, glucose is either diverted from the pathway that generates fructose and/or fructose is consumed under reaction conditions. Both are implicated by the kinetic traces in Figures 1 and 4, and the fructose bimolecular reaction observed in Figure 5. Fructose decomposes more readily than glucose,[61] likely due to the relative stability of the pyranose versus furanose forms of the sugars. The effect of fructose decomposition is particularly pronounced at high pH_o.

DOI: 10.1021/acscatal.5b00316
ACS Catal. 2015, 5, 3162−3173

Scheme 3. Proposed Mechanism for Isomerization of Glucose to Fructose[a]

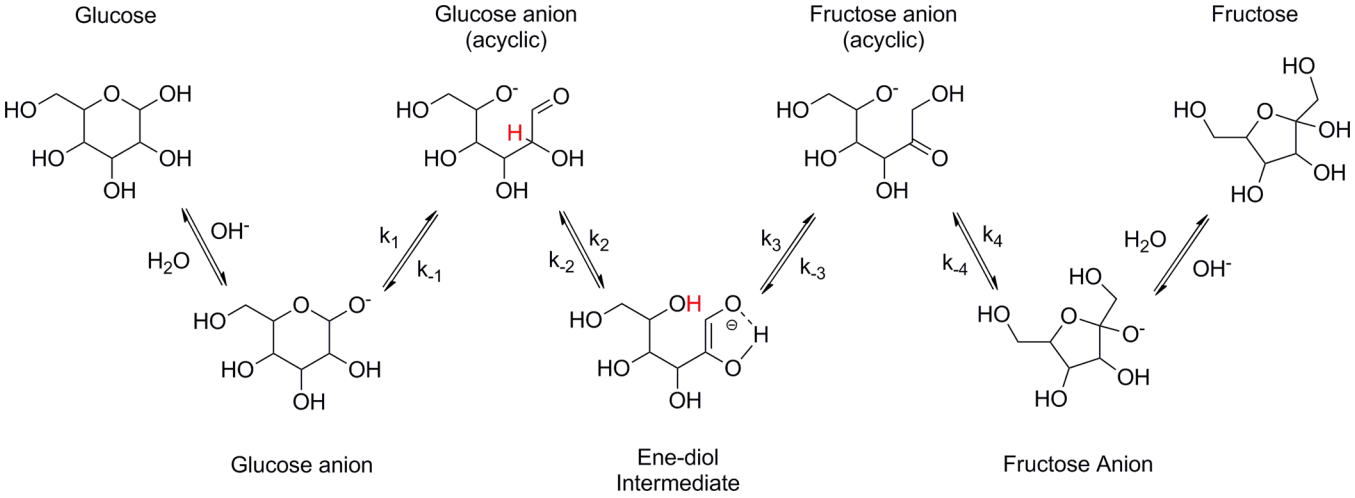

[a]Mannose was omitted for clarity.

Scheme 4. Decomposition Pathways in Base-Catalyzed Isomerization of Glucose to Fructose[a]

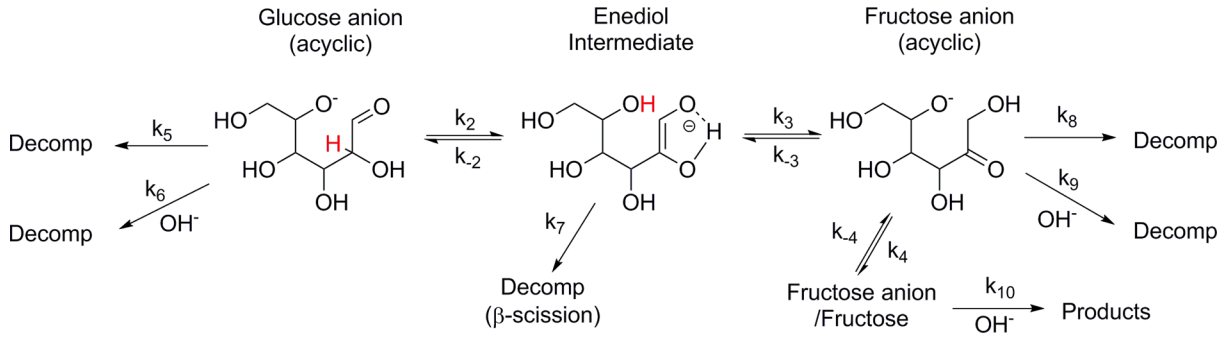

[a]Mannose was omitted for clarity.

Reactive Species Involved in the Isomerization Reaction. We proposed in our previous work[27] a reaction mechanism consistent with the kinetic model summarized by Kooyman et al.[62] in which isomerization occurs after deprotonation of an acyclic form of the sugar. Here, the lack of effect that initial glucose concentration has on k_{obs} (Table 1) supports our previous assessment that glucose conversion is a unimolecular process (Scheme 3). The pH dependence of k_{obs} (Figure 2) suggests ring opening from glucose anions and requires expression of $[Glu^-]$ as a function of $[OH^-]$ and $[Glu]_{total}$ in the rate law to take this effect into account (eq 6 and Supporting Information). This is consistent with many previous works carried out under high concentrations of inorganic bases and having no dependence on $[OH^-]$.[20,24] Under such extreme conditions, $[OH^-] \gg Kb_{Glu}$ and the first term in eq 6 simplifies to $-k_1[Glu]_{total}$. Under our experimental conditions, a distinction cannot be made between deprotonation of acyclic glucose followed by intramolecular proton transfer proposed by de Wit et al.[20] (Scheme 3) or proton abstraction by an external base (Scheme 2) due to the multiple pathways by which intermediates may react. As a result, the two reaction pathways are kinetically difficult to distinguish without going to the extremes of high $[OH^-]$. However, at such extremes, the side reactions will likely become too overwhelming to make clear distinctions. A strong argument can be made in favor of the intramolecular pathway, as will be discussed in more detail below. Additionally, rate constants and product distributions obtained with piperidine, pyrrolidine, and NaOH at iso-pH_o (11.0) were similar to TEA, except the contribution from bimolecular Maillard browning for secondary amines. The similarity in k_{obs} between NaOH and TEA indicates that conversion of glucose is not dependent on the structure and/or pK_a of the external base; the basic species involved in the reaction are the hydroxide ions (OH^-) generated in situ through interaction between the amine and water. Similar observations have been made with tetramethylguanidine and NaOH.[40] Product distributions and k_{obs} for the reverse reaction are similar for TEA and NaOH, Table 5, entries 6–7. This also supports that OH^- is the unidentified reactant "X" in eq 4 and that the bimolecular reaction likely describes the alkaline degradation of fructose (e.g., the formation of carboxylic acids from fructose though nucleophilic attack of OH^-).[33,52,53]

$$\frac{d[Glu^-]}{dt} = -k_1[Glu^-] + k_{-1}[Glu^-_{open}] = -k_1\frac{[OH^-][Glu]_{total}}{Kb_{Glu} + [OH^-]} + k_{-1}[Glu^-_{open}] \quad (6)$$

$$\frac{d[Glu^-_{open}]}{dt} = -(k_{-1} + k_2 + k_5 + k_6[OH^-])[Glu^-_{open}] + k_1[Glu^-] + k_{-2}[ED] \quad (7)$$

DOI: 10.1021/acscatal.5b00316
ACS Catal. 2015, 5, 3162–3173

$$\frac{d[ED]}{dt} = -(k_{-2} + k_3 + k_7)[ED] + k_2[Glu^-_{open}] + k_{-3}[Fru^-_{open}] \quad (8)$$

$$\frac{d[Fru^-_{open}]}{dt} = -(k_{-3} + k_4 + k_8 + k_9[OH^-])[Fru^-_{open}] + k_3[ED] + k_{-4}[Fru^-] \quad (9)$$

$$\frac{d[Fru^-]}{dt} = -(k_{-4} + k_{10}/Kb_{Fru})[Fru^-] + k_4[Fru^-_{open}] \quad (10)$$

Isotope Effects and Competitive Reactions. Although earlier isotope labeling experiments report a variety of results that are somewhat ambiguous when compared,[20,23,24,29,32,54] the results in this investigation offer a great deal of insight into the mechanisms presented in Schemes 3 and 4. The effect of replacing H with D at the C-2 position in glucose is substantial (k_H/k_D = 3.8). The following conclusions can be drawn: (i) deprotonation of acyclic glucose occurs prior to the rate limiting step, evidenced by a k_{ie} of 3.8 observed in the kinetics. (ii) The significant decrease in glucose conversion and fructose yield upon retarding enediol formation (Scheme 4, k_2) indicates that a competition exists between deprotonation (k_2) and decomposition of the acyclic form (Scheme 4, k_5, k_6). (iii) This competition strongly favors formation of the enediol intermediate when isomerizing proteo-glucose (glu-C2-H), which is supported by the relative product distributions after short reaction times. Fructose selectivity of 78% was obtained from glu-C2-H (pH_o 10.9, 100 °C, 3 min) compared to only 45% from glu-C2-D under the same conditions. Additionally, fructose selectivities up to 91% were observed after 2 min at 100 °C, pH_o = 11.5. The final mechanistic detail that the labeling experiments reveal is (iv) one of the pathways by which acidic byproducts are formed is decomposition from acyclic glucose. The changes in pH after three apparent half-lives with glu-C2-H and glu-C2-D were 1.5 units and 2.0 units, respectively. The more rapid decrease in pH not only resulted in lower fructose yields but also lower glucose conversion (47% glu-H vs 36% glu-D).

The retardation effect on reaction 2 in Scheme 4 resulting from deuteration of glucose most easily explains the changes in product distribution when considering the fate of acyclic glucose. If the formation of the enediol intermediate is the only pathway that leads to fructose, then the probability of its formation can be expressed as $k_2/(k_{-1} + k_2 + k_5 + k_6[OH^-])$. Once glucose has undergone ring opening to the acyclic form, this intermediate is consumed by one of four reactions: (i) ring closing (k_{-1}), (ii) deprotonation to the enediol (k_2), (iii) thermal decomposition (k_5), and (iv) nucleophilic attack by OH^- ($k_6[OH^-]$). All of these reactions are supported by the isotopically labeled experiment, pH effects, or literature studies on decomposition[25,33,38,39,52,53] and ring opening/closing.[20,22,42−46] Once the enediol intermediate is generated, a similar competition takes place: (i) rearrangement to acyclic fructose (k_3), (ii) reformation of acyclic glucose (k_{-2}), or (iii) decomposition (likely through β-scission, k_7).[20] The probability of successful formation of acyclic fructose is therefore $k_3/(k_{-2} + k_3 + k_7)$. Competition for the resulting acyclic fructose now begins and essentially mirrors that of glucose. The probability of successful ring closing to fructose anion and eventually neutral fructose is $k_{-3}/(k_{-3} + k_4 + k_8 + k_9[OH^-])$; however, unlike glucose (which is relatively stable in its neutral ring form), fructose can undergo a bimolecular reaction with OH^- which may lead to either decomposition or bimolecular ring opening[22] ultimately returning to glucose. Finally, the fact that all of these reactions (except for decomposition) are reversible and have similar forward and reverse rate constants ($K_{overall} = k_{forward}/k_{reverse}$ = 1.348 at 100 °C)[7] is an additional hindrance to high fructose yields. In light of this analysis, it is easy to understand why this reaction system is so challenging and why most works reported low selectivities to fructose. Clearly, temperature and pH have significant effects on the reaction pathways and therefore yields. Of equal importance is the residence time of the sugars under these reaction conditions as repeated cycling between glucose and fructose results in degradation through the intermediates, thus consumption of the carbohydrates. This can be easily seen when calculating the carbon balance (taking only the sugars into account) as a function of time, as it decreased from 92% to 84% when extending the reaction time from 5 to 15 min. During that 10 min time span, fructose yields only increased by an additional 1−2% at most. Interestingly, the carbon balance at 30 min calculated for TEA (79%) was similar to the value obtained for Sn-β (84%), thus indicating that similar levels of sugar degradations can be expected for Lewis acids.

Intramolecular vs Bimolecular Deprotonation. Although the results indicate that deprotonation occurs from acyclic forms of the sugars, it is not obvious which species is responsible for accepting the proton—for example, intramolecular proton transfer (deprotonation of C-2, protonation of O-5; reaction 2 of Scheme 3) or bimolecular deprotonation with OH^- followed by reprotonation from H_2O (Scheme 2). The results obtained for glu-C2-H in D_2O are somewhat ambiguous. If deprotonation of acyclic forms of the sugars is a bimolecular reaction, and reprotonation occurs from the solvent, then a solvent k_{ie} = 1 could suggest that either (i) reprotonation of the enediol is post-rate-limiting step (as one would expect to observe a kinetic isotope effect from the solvent) or (ii) deprotonation of the enediol is an intramolecular process and, therefore, does not involve the solvent. Unfortunately, no such distinction can be made from these results. However, considering the extreme conditions (high $[OH^-]$) in regards to the above proposed reaction mechanism, one would expect to see the following. If OH^- is responsible for deprotonation of acyclic sugar as shown in Scheme 2, then k_2 and k_{-3} should exhibit first-order dependence on $[OH^-]$. Therefore, in the limit of high $[OH^-]$, the term $k_2[OH^-]/(k_{-1} + k_2[OH^-] + k_5 + k_6[OH^-])$ simplifies to $k_2/(k_2 + k_6)$. As a result, fructose yields would be expected to plateau. To the contrary, an intramolecular deprotonation event (having no dependence on $[OH^-]$) would yield $k_2/(k_6[OH^-])$ at high $[OH^-]$. Infinitely high $[OH^-]$ would favor direct decomposition (k_6) without formation of enediol intermediate and therefore no formation of fructose. Admittedly, these treatments are oversimplified. They do not take into account competing reactions for other intermediates or bimolecular decay of fructose, but the low yields reported in the literature at high $[OH^-]$ anecdotally support intramolecular proton abstraction. Additionally, a marked decrease in fructose yields and increase in degradation products were reported during base-catalyzed isomerization as the ratio of NaOH to glucose was increased from 0.12 to 1.00.[40] On the other hand, strictly invoking intramolecular proton transfer (reversible proton transfer exclusively between C-2 and O-5) does not allow for the incorporation or loss of deuterium or tritium observed in some of the isotopically labeled experiments.[20,23,24,29,32,54] Even the large negative entropy of activation for the unimolecular

DOI: 10.1021/acscatal.5b00316
ACS Catal. 2015, 5, 3162−3173

process calculated in this work could either suggest bimolecular deprotonation from acyclic sugars or significant solvent rearrangement as a result of ring cleavage. Perhaps the inconsistencies observed in the earlier isotope labeling experiments[20,23,24,29,32,54] point to parallel pathways by which the fraction of deprotonation/reprotonation by either the intramolecular reaction or by OH^- is dependent on temperature (thus varying the ratio of the elementary rate constants for each reaction $\{k_{intra}/k_{OH}\}$) and $[OH^-]$ thereby varying the ratio of the apparent rate constants for each step $(k_{intra}/\{k_{OH}[OH^-]\})$.

Activation Parameters. Because the rate constants measured for unimolecular fructose reaction and the glucose reaction are a composite of forward and reverse rate constants for the same isomerization, they are expected to be similar. Indeed, the plot of $\ln(k/T)$ versus $1/T$ shown in Figure 3 reveals statistically identical activation parameters.

Large negative values of $\Delta S^{\ddagger}$ are typically observed as a result of bimolecular reactions (k_{bimol} $\Delta S^{\ddagger} = -274$ J/molK). However, other results clearly show that the isomerization is a unimolecular reaction with respect to the monosaccharide. Therefore, the large negative $\Delta S^{\ddagger}$ (ca. −140 J/molK) observed for the unimolecular pathways here may be due to a portion of the intermediates reacting with OH^- and/or substantial rearrangement of solvent molecules to accommodate the intermediates. Calculated activation energies for ring opening of monosaccharides vary substantially upon the inclusion of a single water molecule.[46,63]

Analogies and Differences with Lewis Acids. The catalytic performance of this isomerization system is similar to Sn-β in several ways: turnover rates (0.018 ± 0.01 mol_{Fru} s^{-1} mol_{TEA}^{-1} at 100 °C) versus Sn-β (0.027 mol_{Fru} s^{-1} mol_{Sn}^{-1} at 100 °C),[12] mass balance (both ∼84% at prolonged reaction times), fructose yields (32% TEA vs 31% Sn-β), and selectivity (64% TEA vs 51% Sn-β). Both systems produce sugar derived carboxylic acids which play a role in catalyst deactivation, but unlike Sn-β,[16] the deactivation of the TEA system is a result of reversible protonation of the base. Additionally, the activation energy for Sn-β (93 kJ/mol) at 100 °C is substantially higher than the base-catalyzed route measured in this work (61 kJ/mol).

CONCLUSIONS

In light of the disadvantages of enzyme-catalyzed glucose isomerization (cost, sensitivity to feed purity, irreversible deactivation, etc.), many researchers have put considerable efforts in developing and understanding novel isomerization catalysts. Early studies of Brønsted base-catalyzed glucose isomerization reactions typically resulted in dismally low yields of fructose. However, the majority of these studies were carried out under strongly alkaline conditions. The reaction mechanism under these conditions has been a point of great interest and debate since its initial discovery over a century ago. Although a great deal of progress has been made in understanding the chemistry of base-catalyzed glucose isomerization, high fructose yields have only recently been reported.[27,40] This work investigated the kinetics and product distribution under high fructose yield conditions with consideration to the substantial amount of the work already done in this area in order to better understand the base-catalyzed mechanism and lay the foundation for the synthesis and implementation of novel base catalysts.

When one considers (i) the lack of dependence that fructose yields have on pH_o in the range 10.7 to 11.3, (ii) no conversion expected below pH_o 9,[28] and (iii) the observed decrease in pH with time, it becomes evident that although the equilibrium constants are independent of pH, the degree of reactivity in the system (e.g., glucose conversion) is pH-dependent. As a result, under more basic conditions larger quantities of glucose can be converted to products before the formation of acidic byproducts overwhelms the combined buffering capacity of the glucose, fructose, and TEA in solution. Simultaneously, a high pH environment enhances degradation pathways of ring fructose and acyclic forms of both sugars, thus stifling yields. An ideal system is one in which glucose is introduced to a high pH (∼11.3) environment at high temperature for a short period of time so that each molecule participates in the isomerization cycle only one time. As a result, losses due to degradation of acyclic forms of the sugars will be minimized. In addition, fructose should be removed from the reaction system immediately upon formation to avoid the observed bimolecular reaction.

ASSOCIATED CONTENT

Supporting Information

The following file is available free of charge on the ACS Publications website at DOI: 10.1021/acscatal.5b00316.

Detailed UPLC methods, amine screening results with and without the exclusion of CO_2, catalyst performance for fructose to glucose isomerization as a function of pH, and NMR spectra (PDF)

AUTHOR INFORMATION

Corresponding Author

*E-mail: tesso@iastate.edu. Phone +1 515-294-4595.

Notes

The authors declare no competing financial interest.

ACKNOWLEDGMENTS

This material is based upon work supported in part by Iowa State University and the National Science Foundation Grant Numbers EEC-0813570 and EPSC-1101284. The authors would like to thank Mr. Chi (Alex) Liu and Mrs. Sarah Curry for their assistance in experimental preparation and insightful discussions, as well as Dr. Sarah Cady (ISU Chemical Instrumentation Facility) for training and assistance pertaining to the AVIII-600 results included in this publication.

REFERENCES

(1) Climent, M. J.; Corma, A.; Iborra, S. *Green Chem.* **2014**, *16*, 516−547.
(2) Wang, T.; Nolte, M. W.; Shanks, B. H. *Green Chem.* **2014**, *16*, 548−572.
(3) van Putten, R.-J.; van der Waal, J. C.; de Jong, E.; Rasrendra, C. B.; Heeres, H. J.; de Vries, J. G. *Chem. Rev.* **2013**, *113*, 1499−1597.
(4) Bhosale, S. H.; Rao, M. B.; Deshpande, V. P. *Microbiol. Rev.* **1996**, *60*, 280−300.
(5) Misset, O. In *Handbook of Food Enzymology*; Whitaker, J. R., Voragen, A. G. J., Wong, D. W. S., Eds.; Marcel Dekker: New York, 2003; pp 1057−1077.
(6) Buchholz, K.; Seibel, J. *Carbohydr. Res.* **2008**, *343*, 1966−1979.
(7) Tewari, Y. B.; Goldberg, R. N. *Appl. Biochem. Biotechnol.* **1985**, *11*, 17−24.
(8) Aider, M.; Halleux, D. d. *Trends Food Sci. Technol.* **2007**, *18*, 356−364.

DOI: 10.1021/acscatal.5b00316
ACS Catal. 2015, 5, 3162−3173

(9) Zhao, S.; Guo, X.; Bai, P.; Lv, L. *Asian J. Chem.* **2014**, *26*, 4537−4543.
(10) Moliner, M.; Román-Leshkov, Y.; Davis, M. E. *Proc. Natl. Acad. Sci. U. S. A.* **2010**, *107*, 6164−6168.
(11) Bermejo-Deval, R.; Assary, R. S.; Nikolla, E.; Moliner, M.; Román-Leshkov, Y.; Hwang, S.-J.; Palsdottir, A.; Silverman, D.; Lobo, R. F.; Curtiss, L. A.; Davis, M. E. *Proc. Natl. Acad. Sci. U. S. A.* **2012**, *109*, 9727−9732.
(12) Bermejo-Deval, R.; Gounder, R.; Davis, M. E. *ACS Catal.* **2012**, *2*, 2705−2713.
(13) Bermejo-Deval, R.; Orazov, M.; Gounder, R.; Hwang, S.-J.; Davis, M. E. *ACS Catal.* **2014**, *4*, 2288−2297.
(14) Caratzoulas, S.; Davis, M. E.; Gorte, R. J.; Gounder, R.; Lobo, R. F.; Nikolakis, V.; Sandler, S. I.; Snyder, M. A.; Tsapatsis, M.; Vlachos, D. G. *J. Phys. Chem. C* **2014**, *118*, 22815−22833.
(15) Li, Y.-P.; Head-Gordon, M.; Bell, A. T. *ACS Catal.* **2014**, *4*, 1537−1545.
(16) Rajabbeigi, N.; Torres, A. I.; Lew, C. M.; Elyassi, B.; Ren, L.; Wang, Z.; Je Cho, H.; Fan, W.; Daoutidis, P.; Tsapatsis, M. *Chem. Eng. Sci.* **2014**, *116*, 235−242.
(17) Choudhary, V.; Pinar, A. B.; Lobo, R. F.; Vlachos, D. G.; Sandler, S. I. *ChemSusChem* **2013**, *6*, 2369−2376.
(18) Román-Leshkov, Y.; Moliner, M.; Labinger, J. A.; Davis, M. E. *Angew. Chem., Int. Ed.* **2010**, *49*, 8954−8957.
(19) Rai, N.; Caratzoulas, S.; Vlachos, D. G. *ACS Catal.* **2013**, *3*, 2294−2298.
(20) de Wit, G.; Kieboom, A. P. G.; van Bekkum, H. *Carbohydr. Res.* **1979**, *74*, 157−175.
(21) Despax, S.; Estrine, B.; Hoffmann, N.; Le Bras, J.; Marinkovic, S.; Muzart, J. *Catal. Commun.* **2013**, *39*, 35−38.
(22) Goux, W. J. *J. Am. Chem. Soc.* **1985**, *107*, 4320−4327.
(23) Isbell, H. S.; Frush, H. L.; Wade, C. W. R.; Hunter, C. E. *Carbohydr. Res.* **1969**, *9*, 163−175.
(24) Isbell, H. S.; Linek, K.; Hepner, K. E., Jr *Carbohydr. Res.* **1971**, *19*, 319−327.
(25) Knill, C. J.; Kennedy, J. F. *Carbohydr. Polym.* **2003**, *51*, 281−300.
(26) Lima, S.; Dias, A. S.; Lin, Z.; Brandão, P.; Ferreira, P.; Pillinger, M.; Rocha, J.; Calvino-Casilda, V.; Valente, A. A. *Appl. Catal., A* **2008**, *339*, 21−27.
(27) Liu, C.; Carraher, J. M.; Swedberg, J. L.; Herndon, C. R.; Fleitman, C. N.; Tessonnier, J.-P. *ACS Catal.* **2014**, *4*, 4295−4298.
(28) Simonov, A. N.; Pestunova, O. P.; Matvienko, L. G.; Parmon, V. N. *Russ. Chem. Bull.* **2005**, *54*, 1967−1972.
(29) Sowden, J. C.; Schaffer, R. *J. Am. Chem. Soc.* **1952**, *74*, 505−507.
(30) Speck Jr, J. C. In *Advances in Carbohydrate Chemistry*; Melville, L. W., Ed.; Academic Press: New York, 1958; Vol. *13*, pp 63−103.
(31) Angyal, S. J. In *Glycoscience*; Stütz, A., Ed.; Springer: Berlin, 2001; Vol. *215*, pp 1−14.
(32) Topper, Y. J.; Stetten, D. *J. Biol. Chem.* **1951**, *189*, 191−202.
(33) de Bruijn, J. M.; Kieboom, A. P. G.; van Bekkum, H. *Recl. Trav. Chim. Pays-Bas* **1986**, *105*, 176−183.
(34) Lecomte, J.; Finiels, A.; Moreau, C. *Starch/Staerke* **2002**, *54*, 75−79.
(35) Moreau, C.; Durand, R.; Roux, A.; Tichit, D. *Appl. Catal., A* **2000**, *193*, 257−264.
(36) Román-Leshkov, Y.; Davis, M. E. *ACS Catal.* **2011**, *1*, 1566−1580.
(37) Souza, R. O. L.; Fabiano, D. P.; Feche, C.; Rataboul, F.; Cardoso, D.; Essayem, N. *Catal. Today* **2012**, *195*, 114−119.
(38) Yang, B. Y.; Montgomery, R. *Carbohydr. Res.* **1996**, *280*, 27−45.
(39) Novotný, O.; Cejpek, K.; Velíšek, J. *Czech J. Food Sci.* **2008**, *26*, 117−131.
(40) Jia, S.; Liu, M.; Gong, Y.; Feng, J.; Guo, X. *Acta Pet. Sin., Pet. Process. Sect.* **2012**, *28*, 940−949.
(41) de Bruyn, C. A. L.; van Ehenstein, W. A. *Ber. Dtsch. Chem. Ges.* **1895**, *28*, 3078−3082.
(42) Serianni, A. S.; Pierce, J.; Huang, S. G.; Barker, R. *J. Am. Chem. Soc.* **1982**, *104*, 4037−4044.
(43) Fábián, P.; Asbóth, B.; Náray-Szabó, G. *J. Mol. Struct.: THEOCHEM* **1994**, *307*, 171−178.
(44) Grimshaw, C. E.; Whistler, R. L.; Cleland, W. W. *J. Am. Chem. Soc.* **1979**, *101*, 1521−1532.
(45) Los, J. M.; Simpson, L. B.; Wiesner, K. *J. Am. Chem. Soc.* **1956**, *78*, 1564−1568.
(46) Assary, R. S.; Curtiss, L. A. *Energy Fuels* **2011**, *26*, 1344−1352.
(47) de Bruijn, J. M.; Kieboom, A. P. G.; van Bekkum, H. *J. Carbohydr. Chem.* **1986**, *5*, 561−9.
(48) de Bruijn, J. M.; Kieboom, A. P. G.; van Bekkum, H. *Recl. Trav. Chim. Pays-Bas* **1987**, *106*, 35−43.
(49) de Bruijn, J. M.; Kieboom, A. P. G.; van Bekkum, H. *Starch/Staerke* **1987**, *39*, 23−8.
(50) de Bruijn, J. M.; Kieboom, A. P. G.; van Bekkum, H.; van der Poel, P. W.; de Visser, N. H. M.; de Schutter, M. A. M. *Int. Sugar J.* **1987**, *89*, 190−195.
(51) de Bruijn, J. M.; Touwslager, F.; Kieboom, A. P. G.; van Bekkum, H. *Starch/Staerke* **1987**, *39*, 49−52.
(52) Eggleston, G.; Vercellotti, J. R. *J. Carbohydr. Chem.* **2000**, *19*, 1305−1318.
(53) Shaw, P. E.; Tatum, J. H.; Berry, R. E. *J. Agric. Food Chem.* **1968**, *16*, 979−982.
(54) Fodor, G.; Sachetto, J.-P. *Tetrahedron Lett.* **1968**, *9*, 401−403.
(55) Bothner-By, A. A.; Gibbs, M. *J. Am. Chem. Soc.* **1950**, *72*, 4805−4805.
(56) Corzo-Martínez, M.; Corzo, N.; Villamiel, M.; del Castillo, M. D. In *Food Biochemistry and Food Processing*, 2nd ed.; Simpson, B. K., Nollet, L. M. L., Toldra, F., Benjakul, S., Paliyath, G., Hui, Y. H., Eds.; John Wiley & Sons: Hoboken, NJ, 2012; pp 56−83.
(57) Kim, J.-S.; Lee, Y.-S. *Food Chem.* **2008**, *108*, 582−592.
(58) Wirth, D. D.; Baertschi, S. W.; Johnson, R. A.; Maple, S. R.; Miller, M. S.; Hallenbeck, D. K.; Gregg, S. M. *J. Pharm. Sci.* **1998**, *87*, 31−39.
(59) Sixty-ninth meeting of the Joint FAO/WHO Expert Committee on Food Additives (JECFA). *Safety Evaluation of Certain Food Additives*; World Health Organization: Geneva, 2009; p 155.
(60) U.S. Department of Health and Human Services. *National Toxicology Program - Triethylamine*. http://ntp.niehs.nih.gov/go/12383 (accessed July 28, 2014).
(61) Shallenberger, R. S.; Mattick, L. R. *Food Chem.* **1983**, *12*, 159−165.
(62) Kooyman, C.; Vellenga, K.; De Wilt, H. G. J. *Carbohydr. Res.* **1977**, *54*, 33−44.
(63) Lewis, B. E.; Choytun, N.; Schramm, V. L.; Bennet, A. J. *J. Am. Chem. Soc.* **2006**, *128*, 5049−5058.

DOI: 10.1021/acscatal.5b00316
ACS Catal. 2015, 5, 3162−3173